Chapter 9

Pattern Formation

Patterning is a common occurrence found in a wide variety of physical systems, including chemically active media, fluids far from equilibrium, liquid crystals, *etc.* In this chapter we will touch very briefly on the basic physics of patterning instabilities.

9.0.1 Reaction-Diffusion Dynamics Revisited

Let $\big\{\phi_i(\boldsymbol{r},t)\big\}$ denote a set of scalar fields satisfying

$$\partial_t\,\phi_i + \boldsymbol{\nabla}\cdot\boldsymbol{J}_i = R_i\ , \tag{9.1}$$

where

$$J_i^\alpha = -D_{ij}^{\alpha\beta}\,\partial_\beta\,\phi_j \tag{9.2}$$

is the α component of the current density of species i. We assume that the local reaction kinetics is given by

$$R_i = R_i\big(\{\phi_j\},\lambda\big)\ , \tag{9.3}$$

where λ is a control parameter, or possibly a set of control parameters. Thus,

$$\partial_t\phi_i = \partial_\alpha\,D_{ij}^{\alpha\beta}\,\partial_\beta\,\phi_j + R_i\big(\{\phi_j\},\lambda\big)\ . \tag{9.4}$$

Let us expand about a homogeneous solution to the local dynamics, $R\big(\{\phi_i^*\},\lambda\big)=0$, writing

$$\phi_i(\boldsymbol{r},t) = \phi_i^* + \eta_i(\boldsymbol{r},t)\ . \tag{9.5}$$

We then have

$$\partial_t\,\eta_i = \left.\frac{\partial R_i}{\partial\phi_j}\right|_{\boldsymbol{\phi}^*}\eta_j + \partial_\alpha\,D_{ij}^{\alpha\beta}\,\partial_\beta\,\eta_j\ . \tag{9.6}$$

Assuming $D_{ij}^{\alpha\beta}$ is constant in space, we obtain the linear equation

$$\partial_t\,\hat\eta(\boldsymbol{q},t) = L_{ij}(\boldsymbol{q}\,;\lambda)\,\hat\eta_j(\boldsymbol{q},t)\ , \tag{9.7}$$

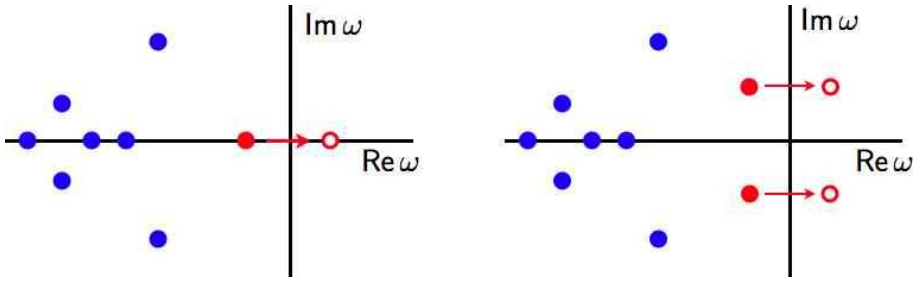

Figure 9.1: Instabilities in linear systems $\dot{\boldsymbol{\eta}} = L\boldsymbol{\eta}$ occur when the real part of the largest eigenvalue of L crosses zero. If L is a real operator, its eigenvalues are either real or come in complex conjugate pairs.

where

$$L_{ij}(\boldsymbol{q}\,;\lambda) = \left.\frac{\partial R_i}{\partial \phi_j}\right|_{\boldsymbol{\phi}^*} - D_{ij}^{\alpha\beta}\, q_\alpha q_\beta \ . \tag{9.8}$$

Let

$$P(\omega) = \det\big(\omega\,\mathbb{I} - L\big) \tag{9.9}$$

be the characteristic polynomial for $L(\boldsymbol{q}\,;\lambda)$. The eigenvalues $\omega_a(\boldsymbol{q}\,;\lambda)$ satisfy $P(\omega_a) = 0$. If we assume that $L_{ij}(\boldsymbol{q}\,;\lambda) \in \mathbb{R}$ is real, then $P(\omega^*) = \big[P(\omega)\big]^*$, which means that the eigenvalues ω_a are either purely real or else come in complex conjugate pairs $\omega_{a,1} \pm i\omega_{a,2}$. The eigenvectors $\psi_i^a(\boldsymbol{q}\,;\lambda)$ need not be real, since L is not necessarily Hermitian. The general solution is then

$$\eta_i(\boldsymbol{q}\,t) = \sum_a C_a\,\psi_i^a(\boldsymbol{q}\,;\lambda)\,e^{\omega_a(\boldsymbol{q}\,;\lambda)\,t} \ . \tag{9.10}$$

Modes with $\mathsf{Re}\,\omega_a > 0$ are stabilized by nonlinear terms, *e.g.* $\dot{A} = rA - A^3$.

Let's assume the eigenvalues are ordered so that $\mathsf{Re}\,(\omega_a) \geq \mathsf{Re}\,(\omega_{a+1})$, and that $\mathsf{Re}\,(\omega_1) \leq 0$ for $\lambda \leq \lambda_{\rm c}$.

- If $\omega_1(\boldsymbol{q} = 0\,;\lambda_{\rm c}) = 0$, we expect a transition between homogeneous ($\boldsymbol{q} = 0$) states at $\lambda = \lambda_{\rm c}$.
- If $\omega_1(\boldsymbol{q} = \boldsymbol{Q}\,;\lambda_{\rm c}) = 0$, we expect a transition to a spatially modulated structure with wavevector $\boldsymbol{Q}$.
- If $\mathsf{Re}\;\omega_1(\boldsymbol{q} = 0\,;\lambda_{\rm c}) = 0$ but $\mathsf{Im}\;\omega_1(\boldsymbol{q} = 0\,;\lambda_{\rm c}) \neq 0$ we expect a Hopf bifurcation and limit cycle behavior.
- If $\mathsf{Re}\;\omega_1(\boldsymbol{q} = \boldsymbol{Q}\,;\lambda_{\rm c}) = 0$ but $\mathsf{Im}\;\omega_1(\boldsymbol{q} = \boldsymbol{Q}\,;\lambda_{\rm c}) \neq 0$ we expect a Hopf bifurcation to a spatiotemporal pattern structure.

In the vicinity of a bifurcation, space and time scales associated with the unstable mode(s) tend to infinity. This indicates a *critical slowing down*. If the unstable modes evolve very slowly, the faster, non-critical modes may be averaged over (*i.e.* 'adiabatically eliminated').

For the most unstable mode $\omega \equiv \omega_1$, we envisage the following possibilities:

$\omega = \epsilon - A\,\boldsymbol{q}^2$	homogeneous states ; $q = 0$ least stable
$\omega = \epsilon - A\big(\boldsymbol{q}^2 - Q^2\big)^2$	modulated: $q = Q$ is least stable
$\omega = \epsilon - A\big(\boldsymbol{q}^2 - Q^2\big)^2 - B\,\boldsymbol{q}^2\,\sin^2\theta_{\boldsymbol{q}}$	$\theta_{\boldsymbol{q}}$ between $\boldsymbol{q}$ and symmetry axis
$\omega = \epsilon - A\,\boldsymbol{q}^2 \pm i\Omega_0$	Hopf, to homogeneous state
$\omega = \epsilon - A\big(\boldsymbol{q}^2 - Q^2\big)^2 \pm i\Omega_0$	Hopf, to modulated state

where

$$\epsilon \propto \frac{\lambda - \lambda_{\rm c}}{\lambda_{\rm c}}\ . \tag{9.11}$$

9.1 Turing and Hopf Instabilities

As an explicit example in $d = 1$ dimension, consider the coupled RDEs,

$$u_t = D_u\,u_{xx} + f(u,v) \tag{9.12}$$
$$v_t = D_v\,v_{xx} + g(u,v)\ . \tag{9.13}$$

We linearize about the fixed point $u = v = 0$, obtaining

$$\begin{pmatrix}\delta\hat{u}_t\\ \delta\hat{v}_t\end{pmatrix} = \overbrace{\begin{pmatrix}f_u - D_u\,q^2 & f_v\\ g_u & g_v - D_v\,q^2\end{pmatrix}}^{L(q)}\begin{pmatrix}\delta\hat{u}\\ \delta\hat{v}\end{pmatrix} + \ldots \tag{9.14}$$

for the Fourier transforms

$$\begin{pmatrix}\delta\hat{u}(q,t)\\ \delta\hat{v}(q,t)\end{pmatrix} = \int\limits_{-\infty}^{\infty}\!dx\,\begin{pmatrix}\delta u(x,t)\\ \delta v(x,t)\end{pmatrix}e^{-iqx}\ . \tag{9.15}$$

We now examine the eigenvalues of L. Clearly we have

$$\mathcal{T} \equiv {\rm Tr}(L) = f_u + g_v - (D_u + D_v)\,q^2 \tag{9.16}$$
$$\mathcal{D} \equiv \det(L) = D_u\,D_v\,q^4 - (D_u\,g_v + D_v\,f_u)\,q^2 + \Delta\ , \tag{9.17}$$

where

$$\Delta = f_u\,g_v - f_v\,g_u \tag{9.18}$$

is the determinant at $q = 0$. The eigenvalues are

$$\omega_\pm = \tfrac{1}{2}\mathcal{T} \pm \sqrt{\tfrac{1}{4}\mathcal{T}^2 - \mathcal{D}}\ . \tag{9.19}$$

Recall that in the $(\mathcal{T},\mathcal{D})$ plane, it is the upper left quadrant, with $\mathcal{T} < 0$ and $\mathcal{D} > 0$, where the fixed point is stable. There are then two instability boundary, both of which are straight

lines. The first boundary is the positive $\mathcal{D}$ axis, *i.e.* $(\mathcal{T} = 0\,, \mathcal{D} > 0)$, which separates the stable spiral from the unstable spiral, corresponding to the onset of an *oscillatory (Hopf) instability*. Since the q^2 term in $\mathcal{T}$ has a negative coefficient[1], this instability first occurs at $q = 0$, *i.e.* in the spatially homogeneous mode. The condition for the Hopf instability is then

$$f_u + g_v = 0 \ . \tag{9.20}$$

The second instability boundary is the half-line $(\mathcal{T} < 0\,, \mathcal{D} = 0)$, which forms the border with the saddle point region. If the coefficient of the q^2 term in $\mathcal{D}$ is negative, *i.e.* if $(D_u\, g_v + D_v\, f_u) > 0$, then the minimum of $\mathcal{D}(q)$ occurs at a finite value, $q = \pm Q$, where

$$Q^2 = \frac{D_u\, g_v + D_v\, f_u}{2 D_u D_v} \ . \tag{9.21}$$

In this case, the instability is to a spatially inhomogeneous state. This is the *Turing instability*. This requires that at least one of f_u and g_v is positive, or *autocatalytic*. However, if both are positive, then the condition for the Hopf instability will already have been satisfied. So for the Turing instability we must require $f_u + g_v < 0$, which says that only one of the species is autocatalytic. Setting $\mathcal{D}(Q) = 0$, we eliminate Q and obtain the condition

$$D_u\, g_v + D_v\, f_u = 2\sqrt{\Delta D_u D_v} \ , \tag{9.22}$$

hence, at the threshold of instability, the ordering wavevector is

$$Q^2 = \sqrt{\frac{\Delta}{D_u D_v}} \ . \tag{9.23}$$

For the Turing instability, we may assume, without loss of generality, that $g_v < 0 < f_u$. The Turing instabilty *preempts* the Hopf instability when eqn. 9.22 is satisfied before eqn. 9.20. It is therefore a necessary (but not sufficient) condition that $D_v > D_u$. *The Turing instability preempts the Hopf instability when only one species is autocatalytic, and the autocatalytic species is less diffusive.* This requires a slowly diffusing *activator* and a more rapidly diffusing *inhibitor*.

9.2 The Brusselator

Consider the so-called Brusselator model of Prigogine and Lefever (1968). The Brusselator is a model for two fictitious chemical reactions,

$$\begin{aligned} \mathrm{A} &\longrightarrow \mathrm{B} \\ 2\mathrm{A} + \mathrm{B} &\longrightarrow 3\mathrm{A} \ . \end{aligned}$$

[1]We assume both diffusion constants are positive: $D_{u,v} > 0$.

The species A is assumed to be supplied and removed from the system, in which case, after adding diffusion, we have two coupled RDEs with

$$f(u,v) = a - (1+b)\,u + u^2 v \tag{9.24}$$

$$g(u,v) = b\,u - u^2 v \ . \tag{9.25}$$

The fixed point $f = g = 0$ occurs at $(u^*, v^*) = (a\,, b/a)$. Linearizing the local dynamics about the fixed point, we obtain

$$\begin{pmatrix} f_u & f_v \\ g_u & g_v \end{pmatrix} = \begin{pmatrix} b-1 & a^2 \\ -b & -a^2 \end{pmatrix} \ . \tag{9.26}$$

Thus, $\Delta = a^2 > 0$. The Hopf instability sets in when $f_u + g_v = 0$, *i.e.* when $b = b_{\rm H}$, where

$$b_{\rm H} = 1 + a^2 \ . \tag{9.27}$$

For the Turing instability, eqn. 9.22 gives $b = b_{\rm T}$, where

$$b_{\rm T} = (1+c)^2 \ , \tag{9.28}$$

where we have defined

$$c \equiv a\sqrt{\frac{D_u}{D_v}} \ . \tag{9.29}$$

Note that $c < a$ for the Turing instability. These two curves intersect at

$$c^* = -1 + \sqrt{1+a^2} \ . \tag{9.30}$$

Note that

$$Q^2 = \frac{a}{\sqrt{D_u D_v}} \qquad \Rightarrow \qquad D_u Q^2 = c \quad , \quad D_v Q^2 = \frac{a^2}{c} \ . \tag{9.31}$$

Suppose we are close to the Turing instability, and we write $b = b_{\rm T} + \epsilon$ with $|\epsilon| \ll 1$. We first expand the coupled RDEs about the fixed point, writing

$$u = u^* + \delta u \tag{9.32}$$

$$v = v^* + \delta v \ , \tag{9.33}$$

with $u^* = a$ and $v^* = \frac{b}{a}$. Written in terms of δu and δv, the coupled RDEs take the form

$$\delta u_t = D_u\,\delta u_{xx} - \delta u + \Big(b\,\delta u + a^2\,\delta v\Big) + \left(\frac{b}{a}\,(\delta u)^2 + 2a\,\delta u\,\delta v + (\delta u)^2 \delta v\right) \tag{9.34}$$

$$\delta v_t = D_v\,\delta v_{xx} - \Big(b\,\delta u + a^2\,\delta v\Big) - \left(\frac{b}{a}\,(\delta u)^2 + 2a\,\delta u\,\delta v + (\delta u)^2 \delta v\right) \ . \tag{9.35}$$

If we ignore the nonlinear terms, we obtain a linear equation which has a solution

$$\delta u(x,t) = U_{11}\,A(t)\,\cos(Qx) \tag{9.36}$$

$$\delta v(x,t) = V_{11}\,A(t)\,\cos(Qx) \ , \tag{9.37}$$

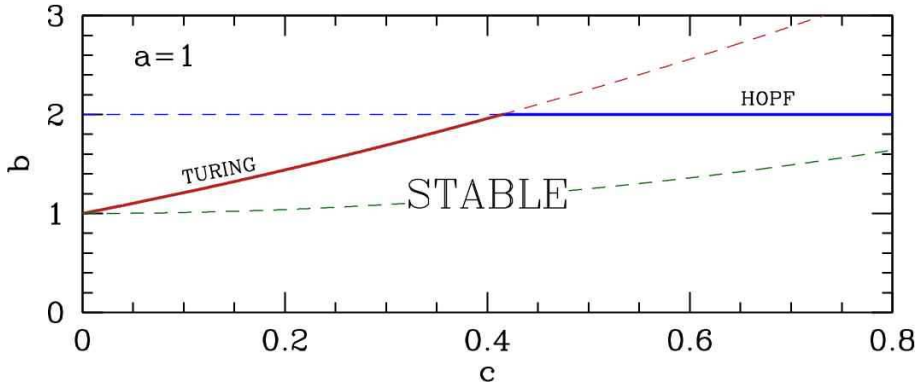

Figure 9.2: Instability lines for the Brusselator. The thick blue line denotes a Hopf instability and the thick red line a Turing instability. The dashed light green line is the locus of points for which $Q^2 > 0$.

where $A(t) = A_0 \exp(\omega t)$ is an amplitude, and where the eigenvector $(U_{11}\ V_{11})^{\rm t}$ satisfies

$$\begin{pmatrix} b-c-1 & a^2 \\ -b & -a^2 - \frac{a^2}{c} \end{pmatrix} \begin{pmatrix} U_{11} \\ V_{11} \end{pmatrix} = \omega \begin{pmatrix} U_{11} \\ V_{11} \end{pmatrix} \ . \tag{9.38}$$

If $b > b_{\rm T}$, then there exists an eigenvalue ω which is real and positive, in which case the amplitude $A(t)$ grows exponentially.

The amplitude equation has a fixed point when $A_t = 0$, which says $\eta = gA^2$.

9.2.1 The amplitude equation

The exponential growth of the amplitude $A(t)$ is valid only insofar as the nonlinear terms in the dynamics are small. Our goal here will be to develop a nonlinear ODE governing the growth of $A(t)$, assuming $|b - b_{\rm T}| \ll 1$. We follow the treatment of Kessler and Levine (2009, unpublished).

We assume one Fourier mode will be excited, with $q = \pm Q$, along with its harmonics. We therefore write

$$\delta u = \sum_{m=1}^{\infty} \sum_{n=0}^{\infty} U_{mn}\, A^m\, \cos(nQx) \tag{9.39}$$

$$\delta v = \sum_{m=1}^{\infty} \sum_{n=0}^{\infty} V_{mn}\, A^m\, \cos(nQx) \ . \tag{9.40}$$

We shall only need the first few terms:

$$\delta u = \big(U_{11}A + U_{31}A^3\big)\cos(Qx) + U_{20}A^2 + U_{22}A^2\cos(2Qx) + \ldots \tag{9.41}$$

$$\delta v = \big(V_{11}A + V_{31}A^3\big)\cos(Qx) + V_{20}A^2 + V_{22}A^2\cos(2Qx) + \ldots \ . \tag{9.42}$$

Note that we assume $U_{10} = V_{10} = 0$ because the leading behavior is in the U_{11} and V_{11} terms. It is through the quadratic nonlinearities that terms with $n = 0$ are generated.

We now undertake the tedious process of working out the RHS of eqns. 9.34 and 9.35 to order A^3. Throughout our derivation, we shall include only the $n = 0$, $n = 1$ and $n = 2$ harmonics and drop all other terms. We will also assume $b = b_{\rm T}$ whenever it multiplies A^m with $m > 1$, since $\epsilon = b - b_{\rm T}$ is presumed small, and, as we shall see, the amplitude itself will be proportional to $\sqrt{\epsilon}$. Let's roll up our sleeves and get to work!

The first terms we need are all the ones linear in δu and δv. Thus, we need

$$D_u\,\delta u_{xx} - \delta u = -(1+c)\Big(U_{11}A + U_{31}A^3\Big)\cos(Qx) - U_{20}A^2 - (1+4c)\,U_{22}A^2\cos(2Qx) \tag{9.43}$$

$$D_v\,\delta v_{xx} = -\frac{a^2}{c}\left(V_{11}A + V_{31}A^3\right)\cos(Qx) - \frac{4a^2}{c}\,V_{22}A^2\cos(2Qx) \tag{9.44}$$

as well as

$$b\,\delta u + a^2\,\delta v = \left\{b\left(U_{11}A + U_{31}A^3\right) + a^2\left(V_{11}A + V_{31}A^3\right)\right\}\cos(Qx) + \Big(b\,U_{20} + a^2\,V_{20}\Big)A^2 + \Big(b\,U_{22} + a^2\,V_{22}\Big)A^2\cos(2Qx)\ . \tag{9.45}$$

Next, we need the nonlinear terms, starting with

$$(\delta u)^2 = \tfrac{1}{2}U_{11}^2A^2 + \tfrac{1}{2}U_{11}^2A^2\cos(2Qx) + U_{11}\big(2\,U_{20} + U_{22}\big)A^3\cos(Qx) + \dots\ , \tag{9.46}$$

where the remaining terms are of $\mathcal{O}(A^4)$ or are proportional to $\cos(3Qx)$. We also require

$$2\,\delta u\,\delta v = U_{11}V_{11}A^2 + U_{11}V_{11}A^2\cos(2Qx) + \Big(2\,U_{11}V_{20} + 2\,V_{11}U_{20} + U_{11}V_{22} + V_{11}U_{22}\Big)A^3\cos(Qx) + \dots\ . \tag{9.47}$$

Finally, we need

$$(\delta u)^2\,\delta v = \tfrac{3}{4}\,U_{11}^2V_{11}\cos(Qx) + \dots\ . \tag{9.48}$$

On the left hand side of eqns. 9.34 and 9.35, we have the time derivative terms. Again, as we shall see, the amplitude A will be proportional to $\sqrt{\epsilon}$, where $\epsilon = b - b_{\rm T}$ is presumed small. Its time derivative A_t will be proportional to $\epsilon^{3/2}$. Therefore, terms such as $(A^2)_t = 2AA_t$ will be negligible and we shall drop them from the outset. Thus,

$$\delta u_t = U_{11}\,A_t\,\cos(Qx) + \dots \tag{9.49}$$

$$\delta v_t = V_{11}\,A_t\,\cos(Qx) + \dots\ . \tag{9.50}$$

The linear terms in A comprise a zero mode for the system with $b = b_{\rm T}$. Thus,

$$\begin{pmatrix} b_{\rm T} - c - 1 & a^2 \\ -b_{\rm T} & -a^2 - \frac{a^2}{c} \end{pmatrix}\begin{pmatrix} U_{11} \\ V_{11} \end{pmatrix} = 0\ . \tag{9.51}$$

We may, without loss of generality, set $U_{11} \equiv 1$. We then have

$$U_{11} = 1 \qquad , \qquad V_{11} = -\frac{c\,(1+c)}{a^2} \ . \tag{9.52}$$

We now set to zero the coefficients of $\cos(nQx)$ for $n = 0$, 1, and 2 in each of eqns. 9.34 and 9.35. Setting the $n = 0$ terms on the RHS of these equations to zero, we obtain

$$U_{20} = 0 \tag{9.53}$$

$$\frac{b}{2a}\,U_{11}^2 + a\,U_{11}V_{11} + a^2\,V_{20} = 0 \ . \tag{9.54}$$

Doing the same for the $n = 2$ terms, we get

$$\frac{b}{2a}\,U_{11}^2 + a\,U_{11}V_{11} + b\,U_{22} + a^2\big(1 + 4c^{-1}\big)V_{22} = 0 \tag{9.55}$$

$$(1+4c)\,U_{22} + \frac{4a^2}{c}\,V_{22} = 0 \ . \tag{9.56}$$

Solving, we obtain

$$U_{20} = 0 \qquad\qquad U_{22} = \frac{2\,(1-c^2)}{9\,ac} \tag{9.57}$$

$$V_{20} = -\frac{1-c^2}{2\,a^3} \qquad\qquad V_{22} = -\frac{(1-c^2)\,(1+4c)}{18\,a^3} \ . \tag{9.58}$$

Finally, we need the $n = 1$ terms. There are three contributions. One comes from the linear terms, restoring the small differences proportional to $\epsilon = b - b_{\rm T}$. These terms contribute a coefficient for $\cos(Qx)$ of $\epsilon\,A$ in the RHS of eqn. 9.34 and $-\epsilon\,A$ on the RHS of eqn. 9.35. A second contribution comes from the nonlinear terms. We invoke eqns. 9.46 and 9.47, multiplying the former by $\frac{b}{a}$ and the latter by a. The term we seek is proportional to $A^3\cos(Qx)$, with a coefficient

$$\frac{b}{a}\,U_{22} + a\,\big(2\,V_{20} + V_{22} + V_{11}U_{22}\big) + \tfrac{3}{4}\,V_{11} = \frac{(1+c)\,(2+c)\,(8c^2-21c+4)}{36\,a^2c} \ . \tag{9.59}$$

We define

$$\lambda = -\frac{(1+c)\,(2+c)\,(8c^2-21c+4)}{36\,a^2c} \ . \tag{9.60}$$

Note that $\lambda > 0$ for $c \in \big[c_-\,,\,c_+\big]$, where $c_\pm = \frac{1}{16}\big(21 \pm \sqrt{313}\,\big)$. Numerically, $c_- \approx 0.20676$ and $c_+ \approx 2.4182$. Finally, we have the U_{31} and V_{31} terms themselves. Thus, dividing out the common $\cos(Qx)$ factor on both sides of both equations, we have

$$A_t = \epsilon\,A + \Big[c\,(1+c)\,U_{31} + a^2\,V_{31} - \lambda\Big]A^3 \tag{9.61}$$

$$-\frac{c\,(1+c)}{a^2}\,A_t = -\epsilon\,A - \Big[(1+c)^2\,U_{31} + \frac{a^2}{c}\,(1+c)\,V_{31} + \lambda\Big]A^3 \ . \tag{9.62}$$

We can rewrite these equations as a linear system for the coefficients U_{31} and V_{31}, *viz.*

$$A^3 \overbrace{\begin{pmatrix} c\,(1+c) & a^2 \\ -(1+c)^2 & -a^2 - \frac{a^2}{c} \end{pmatrix}}^{M} \begin{pmatrix} U_{31} \\ V_{31} \end{pmatrix} = \begin{pmatrix} A_t - \epsilon\,A + \lambda\,A^3 \\ -a^{-2}\,c\,(1+c)\,A_t + \epsilon\,A - \lambda\,A^3 \end{pmatrix} \ . \tag{9.63}$$

In order to be able to satisfy the above equation, the RHS must be orthogonal to the left eigenvector of the matrix M corresponding to the zero eigenvalue. This is called the *solvability condition*. It is easy to see that this zero left eigenvector is proportional to

$$\phi = \begin{pmatrix} 1+c & c \end{pmatrix} \ . \tag{9.64}$$

Thus, we demand

$$(1+c)\Big(A_t - \epsilon\,A + \lambda\,A^3\Big) - c\,\Big(a^{-2}\,c\,(1+c)\,A_t - \epsilon\,A + \lambda\,A^3\Big) = 0 \ . \tag{9.65}$$

This, at long last, yields our amplitude equation:

$$A_t = \eta A - g A^3 \ , \tag{9.66}$$

where

$$\eta = \frac{a^2\,(b - b_{\rm T})}{(1+c)\,(a^2 - c^2)} \qquad , \qquad g = -\frac{a^2\,(2+c)\,(8c^2 - 21c + 4)}{36\,a^2\,c\,(a^2 - c^2)} \ . \tag{9.67}$$

Since $c < a$, we have that η is positive for $b > b_{\rm T}$ and negative for $b < b_{\rm T}$. Furthermore g is positive for $c \in \big[c_-\,,\,c_+\big]$ and negative outside this region. Thus, A has a fixed point $A^* = \sqrt{\eta/g}$ (in addition to the one at $A = 0$) if both η and g are positive, or if both η and g are negative. In the former case, $A = 0$ is unstable and $A = A^*$ is stable. In the latter case, $A = 0$ is stable and $A = A^*$ is unstable.

9.3 Rayleigh-Bénard Instability

Consider a layer of fluid between two horizontal plates, as depicted in fig. 9.3. The top plate is held at temperature T_1 and the bottom plate at temperature T_2, with $\Delta T = T_2 - T_1 > 0$. As the fluid near the bottom plate is heated, it expands, and an upward buoyancy force per unit volume $f_{\rm buoy} = \rho g\,\alpha\,\Delta T$ results, where $\alpha = \frac{1}{V}\frac{\partial V}{\partial T}$ is the thermal expansion coefficient and ρ is the fluid density. This buoyancy force is a destabilizing effect, and is opposed by a stabilizing dissipative force per unit volume $f_{\rm diss} = \nu\kappa\rho/d^3$, where ν is the kinematic viscosity, κ the thermal diffusivity, and d the distance between the plates. The dimensionless ratio of these two force densities is known as the *Rayleigh number*,

$$\mathcal{R} = \frac{f_{\rm buoy}}{f_{\rm diss}} = \frac{g\,d^3\,\alpha\,\Delta T}{\nu\,\kappa} \ . \tag{9.68}$$

When $\mathcal{R} > \mathcal{R}_{\rm c} \approx 1708$, the destabilizing effects are sufficient to destroy the homogeneous state. Due to mass conservation, the entire fluid cannot rise uniformly, hence the instability

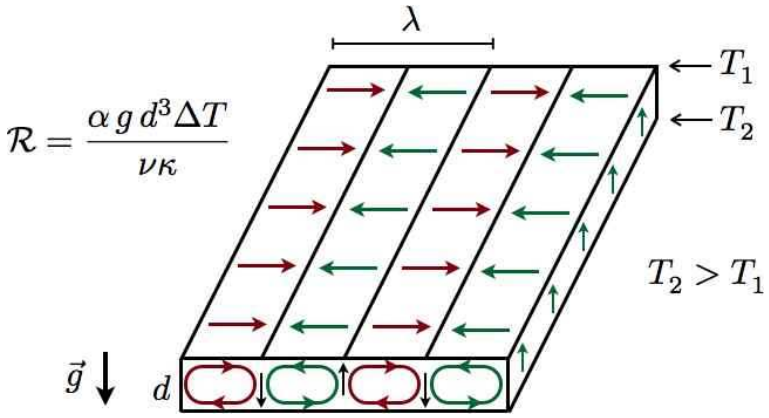

Figure 9.3: Bénard convection cells in a fluid heated from below.

occurs at a finite wavelength λ, owing to the formation of *convective rolls* known as *Bénard cells* (see fig. 9.3).

Swift and Hohenberg (1977) showed that the dynamics for this problem reduces to the following equation for the real field $\sigma(\boldsymbol{r},t)$[2]:

$$\frac{\partial\sigma}{\partial t} = \Big[\varepsilon - \big(Q^2 + \boldsymbol{\nabla}^2\big)^2\Big]\sigma - \sigma^3 \ . \tag{9.69}$$

Here,

$$\varepsilon \propto \mathcal{R} - \mathcal{R}_{\rm c} \tag{9.70}$$

measures the distance from the instability, and $\boldsymbol{\nabla} = \hat{\boldsymbol{x}}\,\partial_x + \hat{\boldsymbol{y}}\,\partial_y$ is the in-plane gradient. Distances are measured in units of d, and the maximally unstable wavevector is $Q \approx 3.12$.

We assume a plane wave disturbance, and we first separate out the oscillating features of $\sigma(\boldsymbol{r},t)$ so that we may talk of a slowly varying amplitude function $A(\boldsymbol{r},t)$:

$$\sigma(\boldsymbol{r},t) = A(\boldsymbol{r},t)\,e^{iQx} + A^*(\boldsymbol{r},t)\,e^{-iQx} \ , \tag{9.71}$$

where $\hat{\boldsymbol{n}}$ is a unit vector which we henceforth assume to be $\hat{\boldsymbol{n}} = \hat{\boldsymbol{x}}$. We then have

$$\sigma^3 = A^3\,e^{3iQx} + 3\,|A|^2\,A\,e^{iQx} + 3\,|A|^2\,A^*\,e^{-iQx} + A^{*3}\,e^{-3IQx} \tag{9.72}$$

$$\big(Q^2 + \boldsymbol{\nabla}^2\big)\,A\,e^{iQx} = e^{iQx}\cdot\big(2iQ\,\partial_x + \partial_x^2 + \partial_y^2\big)A \ . \tag{9.73}$$

Matching coefficients of e^{iQx}, we find

$$\partial_t\,A = \left\{\varepsilon - \Big(2iQ\,\partial_x + \partial_x^2 + \partial_y^2\Big)^2\right\}A - 3\,|A|^2\,A \ . \tag{9.74}$$

If we assume that the solution for A is such that $\partial_x \propto \epsilon^{1/2}$ and $\partial_y \propto \epsilon^{1/4}$ when acting on A, then the ∂_x^2 term is subleading relative to $Q\,\partial_x$ and ∂_y^2, and we may drop it for $|\epsilon| \ll 1$ and write

$$\partial_t\,A = \left\{\varepsilon - \Big(2iQ\,\partial_x + \partial_y^2\Big)^2\right\}A - 3\,|A|^2\,A \ . \tag{9.75}$$

[2]The field σ is actually a combination of temperature and vertical velocity fields.

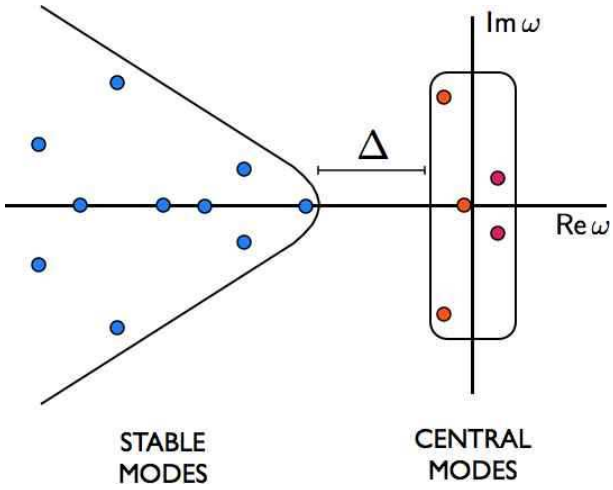

Figure 9.4: Sketch showing separation of frequency scales owing to gap Δ. The fast, stable modes are to the left, and the slow central modes all have $\mathsf{Re}\,\omega_a \approx 0$.

For $\varepsilon > 0$ there is a family of stationary solutions of the form

$$A(x,y) = A_{\boldsymbol{q}}\, e^{i\boldsymbol{q}\cdot\boldsymbol{r}}\, e^{i\delta} \ , \tag{9.76}$$

where

$$A_{\boldsymbol{q}} = \frac{1}{\sqrt{3}}\Big(\varepsilon - \big(2Qq_x + q_y^2\big)^2\Big)^{1/2} \ . \tag{9.77}$$

The instability first occurs at $\boldsymbol{q} = 0$, at $\varepsilon = 0$. As we shall see, the nonlinearity severely limits what multimode structures may form.

The derivation of the Swift-Hohenberg equation utilizes something called the *Boussinesq approximation*, in which the density variation of the fluid enters only in the buoyancy equation. For *non-Boussinesq* fluids, the symmetry $\sigma \to -\sigma$ is broken, and one has

$$\partial_t\,\sigma = \Big[\varepsilon - \big(Q^2 + \boldsymbol{\nabla}^2\big)^2\Big]\sigma + v\,\sigma^2 - \sigma^3 \ , \tag{9.78}$$

for which the bifurcation is subcritical. This is called the *Haken model*.

9.4 Center Manifold Reduction

Consider a dynamical system in the vicinity of a fixed point: $\dot\phi_i = L_{ij}\,\phi_j + \mathcal{O}(\phi^2)$. If we expand the variables ϕ_i in terms of the eigenvectors ψ_i^a of L, writing $\phi_i = \sum_a A_a\,\psi_i^a$, then we can treat the A_a as new variables. Furthermore, we assume that the eigenspectrum $\{\omega_a\}$ exhibits a gap Δ, as shown in fig. 9.4, which allows us to classify these normal modes as either stable or central. The stable normal modes have large ($\mathsf{Re}\ \omega_a < -\Delta$) negative real parts to their frequencies, and hence relax rapidly. On this time scales $\tau \lesssim \Delta^{-1}$, the

central modes are roughly constant. We label these modes as $A^{\rm c}_a$ and $A^{\rm s}_a$, respectively. The dynamics of these modes may be written as

$$\frac{dA^{\rm c}_a}{dt} = J_{ab}\,A^{\rm c}_b + M_a(\boldsymbol{A}^{\rm c},\boldsymbol{A}^{\rm s}) \tag{9.79}$$

$$\frac{dA^{\rm s}_a}{dt} = K_{ab}\,A^{\rm s}_b + N_a(\boldsymbol{A}^{\rm c},\boldsymbol{A}^{\rm s})\ , \tag{9.80}$$

where M_a and N_a are nonlinear. If we assume that the fast, stable modes come to equilibrium, we set $\dot A^{\rm s}_a = 0$ and solve the nonlinear equations $K_{ab}A^{\rm s}_b + N_a(\boldsymbol{A}^{\rm c},\boldsymbol{A}^{\rm s}) = 0$ to obtain $A^{\rm s}_a = A^{\rm s}_a(\boldsymbol{A}^{\rm c})$. Inserting this into the first of the previous sets of equations, we arrive at a new set of equations for the central modes alone. These new equations, obtained by substituting the solution for the stable modes, which are slaved to the slower central modes, into the function $M_a(\boldsymbol{A}^{\rm c},\boldsymbol{A}^{\rm s})$, are of the form

$$\frac{dA^{\rm c}_a}{dt} = L_{ab}\,A^{\rm c}_b + P_a(\boldsymbol{A}^{\rm c})\ . \tag{9.81}$$

where P_a is nonlinear.

It is convenient to consider a nonlinear change of variables $(\boldsymbol{A}^{\rm c},\boldsymbol{A}^{\rm s}) \to (\boldsymbol{B}^{\rm c},\boldsymbol{B}^{\rm s})$ so that the center manifold is described by $\boldsymbol{B}^{\rm s} = 0$. To this end, we write $\boldsymbol{B} = \boldsymbol{A} + \boldsymbol{F}(\boldsymbol{A})$, or, equivalently, $\boldsymbol{A} = \boldsymbol{B} + \boldsymbol{G}(\boldsymbol{B})$. Note that to linear order the transformation is the identity $\boldsymbol{A} = \boldsymbol{B}$ because we wish to preserve the identification of the stable and central modes.

As a simple example, consider the system

$$\frac{dA_1}{dt} = 2A_1A_2 \tag{9.82}$$

$$\frac{dA_2}{dt} = -5A_2 - A_1^2\ . \tag{9.83}$$

We identify A_1 as the central mode and A_2 as the stable fast mode. We now try a nonlinear transformation of the form

$$A_1 = B_1 + \alpha\,B_1^2 + \beta\,B_1B_2 + \gamma\,B_2^2 \tag{9.84}$$

$$A_2 = B_2 + \alpha'\,B_1^2 + \beta'\,B_1B_2 + \gamma'\,B_2^2\ . \tag{9.85}$$

We then have

$$\frac{dA_2}{dt} = \frac{dB_2}{dt} + 2\alpha'\,B_1\,\frac{dB_1}{dt} + \beta'\,B_1\,\frac{dB_2}{dt} + \beta'\,B_2\,\frac{dB_1}{dt} + 2\gamma'\,B_2\,\frac{dB_2}{dt}\ . \tag{9.86}$$

Setting $\beta' = 0$ we obtain the equation

$$\big(1 + 2\gamma' B_2\big)\,\frac{dB_2}{dt} = -5B_2 - (1+5\alpha')\,B_1^2 - 5\gamma'\,B_2^2 + \mathcal{O}(B^3) \tag{9.87}$$

We see that B_2 becomes isolated from B_1 if we choose $\alpha' = -\frac{1}{5}$. We are free to choose any value of γ' we please; for simplicity we choose $\gamma' = 0$. The B_2 equation is then

$$\frac{dB_2}{dt} = -5B_2\ . \tag{9.88}$$

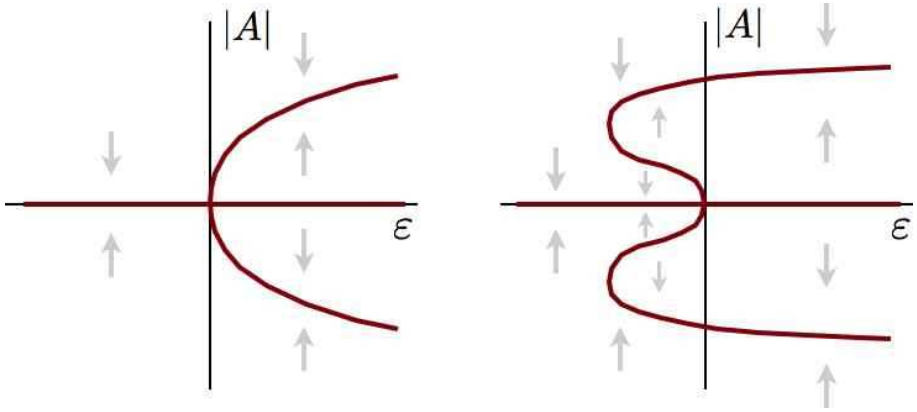

Figure 9.5: Flow diagrams for one-dimensional bifurcations $\dot{A} = \varepsilon\, A - g\,|A|^2 A$ with $g > 0$ (left) and $\dot{A} = \varepsilon\, A - g_1\,|A|^2 A - g_2\,|A|^4 A$ with $g_1 < 0$ and $g_2 > 0$ (right).

The fixed point is $B_2 = 0$. Note that

$$A_2 = B_2 - \tfrac{1}{5} B_1^2 \tag{9.89}$$

and so at the fixed point we conclude

$$A_2 = -\tfrac{1}{5} A_1^2 + \mathcal{O}(A_1^3)\ , \tag{9.90}$$

which is obvious from inspection of eqn. 9.83 as well.

9.5 Selection and Stability of Spatial Patterns

Consider the spatiotemporal dynamics for a real field $\sigma(\boldsymbol{r}, t)$ close to an instability which lies at $|\boldsymbol{q}| = Q$. We assume a form

$$\sigma(\boldsymbol{r}, t) = \sum_{\ell=1}^{M} \Big(A_\ell(t)\, e^{i\boldsymbol{q}_\ell \cdot \boldsymbol{r}} + A_\ell^*(t)\, e^{-i\boldsymbol{q}_\ell \cdot \boldsymbol{r}} \Big)\ , \tag{9.91}$$

where $\boldsymbol{q}_\ell = Q\,\hat{\boldsymbol{n}}_\ell$ and $\hat{\boldsymbol{n}}_\ell^2 = 1$. By assuming $A_\ell = A_\ell(t)$, *i.e.* with no spatial $(\boldsymbol{r})$ dependence, we are considering a system whose spatial structure is 'perfect' and whose growth rate is maximum. We now consider the amplitude equations for the $A_\ell(t)$. Note that the set of allowed wavevectors in the Fourier decomposition of $\sigma(\boldsymbol{r}, t)$ consists of $2M$ elements, which we can order $\big\{\boldsymbol{q}_1\,, \ldots\,, \boldsymbol{q}_M\,, -\boldsymbol{q}_1\,, \ldots\,, -\boldsymbol{q}_M\big\}$. With this ordering, we have $\boldsymbol{q}_{\ell+M} = -\boldsymbol{q}_\ell$ and $A_{\ell+M} = A_\ell^*$, where $1 \le \ell \le M$. We will use indices i, j, *etc.* to refer to the entire set: $1 \le j \le 2M$.

9.5.1 $d = 1$

For systems in one spatial dimension, the amplitude equation is quite limited, since $\hat{\boldsymbol{n}} = \hat{\boldsymbol{x}}$ is the only possibility, and consequently $M = 1$. The simplest case is the logistic type

equation,

$$\frac{dA}{dt} = \varepsilon\, A - g\,|A|^2\, A\ . \tag{9.92}$$

Here, $\varepsilon \propto \lambda - \lambda_{\rm c}$ is a measure of the system's proximity to an instability, where λ is a control parameter. There are fixed points at $A = 0$ and, for $g > 0$, at $|A| = \sqrt{\varepsilon/g}$. Fixed points at finite A are in fact fixed *rings* in the Cartesian space $(\mathsf{Re}\ A\,,\ \mathsf{Im}\, A)$, since the phase of A is undetermined and amplitude remains fixed if the phase is varied globally.

With $g > 0$, eqn. 9.92 describes a *supercritical pitchfork bifurcation*. The flow is sketched in the left panel of fig. 9.5. If $g < 0$, the bifurcation is *subcritical*, and the finite A fixed point occurs for $\varepsilon < 0$ and is unstable. In such a case, we must proceed to the next order in the amplitude equation,

$$\frac{dA}{dt} = \varepsilon\, A - g_1\,|A|^2\, A - g_2\,|A|^4\, A\ , \tag{9.93}$$

with $g_1 < 0$ and $g_2 > 0$. The bifurcation diagram for this equation is sketched in the right panel of fig. 9.5.

9.5.2 Remarks on the amplitude equations for $d > 1$

In dimensions $d > 1$ we have the possibility for nonlinear mixing of K different modes, provided

$$\sum_{j=1}^{K} \boldsymbol{q}_j = Q \sum_{j=1}^{K} \hat{\boldsymbol{n}}_j = 0\ . \tag{9.94}$$

Recall also that A_j is associated with $e^{i\boldsymbol{q}_j\cdot\boldsymbol{r}}$ and A_j^* with $e^{-i\boldsymbol{q}_j\cdot\boldsymbol{r}}$. Under these conditions, the amplitude equations take the following general form:

$$\begin{aligned}\frac{dA_i}{dt} = \varepsilon\, A_i + v \sum_{j,k} A_j^*\, A_k^*\ \delta_{\hat{\boldsymbol{n}}_i+\hat{\boldsymbol{n}}_j+\hat{\boldsymbol{n}}_k\,,\,0} - g\,|A_i|^2 A_i - g{\sum_{j}}' \gamma_{ij}\,|A_j|^2\, A_i \\ - \sum_{j,k,l} \lambda_{ijkl}\, A_j^*\, A_k^*\, A_l^*\ \delta_{\hat{\boldsymbol{n}}_i+\hat{\boldsymbol{n}}_j+\hat{\boldsymbol{n}}_k+\hat{\boldsymbol{n}}_l\,,\,0} + \mathcal{O}(A^4)\ .\end{aligned} \tag{9.95}$$

The prime on the sum indicates that the term with $j = i$ is excluded. Taking the complex conjugate, we obtain the equation with index i replaced by $i + M$. The couplings γ_{ij} and λ_{ijkl} are functions of the relative angles:

$$\gamma_{ij} = \gamma(\hat{\boldsymbol{n}}_i\cdot\hat{\boldsymbol{n}}_j) \tag{9.96}$$

$$\lambda_{ijkl} = \lambda(\hat{\boldsymbol{n}}_i\cdot\hat{\boldsymbol{n}}_j\ ,\ \hat{\boldsymbol{n}}_i\cdot\hat{\boldsymbol{n}}_k\ ,\ \ldots)\ . \tag{9.97}$$

Note that if we associate A_j with $e^{i\boldsymbol{q}_j\cdot\boldsymbol{r}}$ we can define $A_{-j} \equiv A_j^*$, associated with $e^{-i\boldsymbol{q}_j\cdot\boldsymbol{r}}$. Also note that v is a constant independent of j and k because the dot products in that case necessarily are all identical: $\hat{\boldsymbol{n}}_i\cdot\hat{\boldsymbol{n}}_j = \hat{\boldsymbol{n}}_j\cdot\hat{\boldsymbol{n}}_k = \hat{\boldsymbol{n}}_k\cdot\hat{\boldsymbol{n}}_i$.

9.5.3 $d = 2$

For $d = 2$ systems all the allowed wavevectors lie on the circle $|\boldsymbol{q}_j| = Q$. Let's consider the cases $M = 1$, $M = 2$, and $M = 3$.

For $M = 1$ we recapitulate the $d = 1$ case. We have $\boldsymbol{q}_1 = Q\hat{\boldsymbol{x}}$ and $\boldsymbol{q}_2 = -Q\hat{\boldsymbol{x}}$ (up to continuous rotations). The amplitude equation is of the form $\dot{A} = \varepsilon\, A - g\,|A|^2 A$, and the patterned state is one with bands (stripes). This is not the last word, however, since we must check its stability with respect to $M = 2$ and $M = 3$ patterns.

$M = 2$ case

For $M = 2$, we write

$$\sigma(x, y, t) = A_1(t)\, e^{iQx} + A_1^*(t)\, e^{-iQx} + A_2(t)\, e^{iQy} + A_2^*(t)\, e^{-iQy} \ . \tag{9.98}$$

The amplitude equations are

$$\dot{A}_1 = \varepsilon\, A_1 - g\,|A_1|^2 A_1 - \gamma\, g\,|A_2|^2 A_1 \tag{9.99}$$

$$\dot{A}_2 = \varepsilon\, A_2 - g\,|A_2|^2 A_2 - \gamma\, g\,|A_1|^2 A_2 \ . \tag{9.100}$$

We assume $g > 0$. There are four possible fixed points $(\mathcal{A}_1, \mathcal{A}_2)$:

$$\begin{aligned}
&(\mathcal{A}_1, \mathcal{A}_2) = (0\,, 0) && \text{(I: trivial state)} \\
&(\mathcal{A}_1, \mathcal{A}_2) = \sqrt{\varepsilon/g}\,\cdot (e^{i\alpha_1}, 0) && \text{(II: } y\text{-directed bands)} \\
&(\mathcal{A}_1, \mathcal{A}_2) = \sqrt{\varepsilon/g}\,\cdot (0\,,\, e^{i\alpha_2}) && \text{(III: } x\text{-directed bands)} \\
&(\mathcal{A}_1, \mathcal{A}_2) = \sqrt{\varepsilon/g\,(1+\gamma)}\,\cdot (e^{i\alpha_1}, e^{i\alpha_2}) && \text{(IV: squares)}
\end{aligned}$$

Note that $\mathcal{A}_1 \to \mathcal{A}_1\, e^{-i\beta}$ is equivalent to a translation of the pattern in the $\hat{\boldsymbol{x}}$-direction by $\Delta x = \beta/Q$.

To assess the stability of these fixed points, we write

$$A_j = \mathcal{A}_j\,(1 + \eta_j) \ , \tag{9.101}$$

and we find

$$\begin{pmatrix} \dot{\eta}_1 \\ \\ \dot{\eta}_2 \end{pmatrix} = \overbrace{\begin{pmatrix} \varepsilon - 3g\,|\mathcal{A}_1|^2 - \gamma\, g\,|\mathcal{A}_2|^2 & -2\gamma\, g\,|\mathcal{A}_2|^2 \\ \\ -2\gamma\, g\,|\mathcal{A}_1|^2 & \varepsilon - \gamma\, g\,|\mathcal{A}_1|^2 - 3g\,|\mathcal{A}_2|^2 \end{pmatrix}}^{L} \begin{pmatrix} \eta_1 \\ \\ \eta_2 \end{pmatrix} + \mathcal{O}(\eta^2) \ . \tag{9.102}$$

Evaluating L at the four fixed points, we find

$$L_{\rm I} = \begin{pmatrix} \varepsilon & 0 \\ \\ 0 & \varepsilon \end{pmatrix} \qquad , \qquad L_{\rm II} = \begin{pmatrix} -2\varepsilon & 0 \\ \\ -2\gamma\,\varepsilon & (1-\gamma)\,\varepsilon \end{pmatrix} \tag{9.103}$$

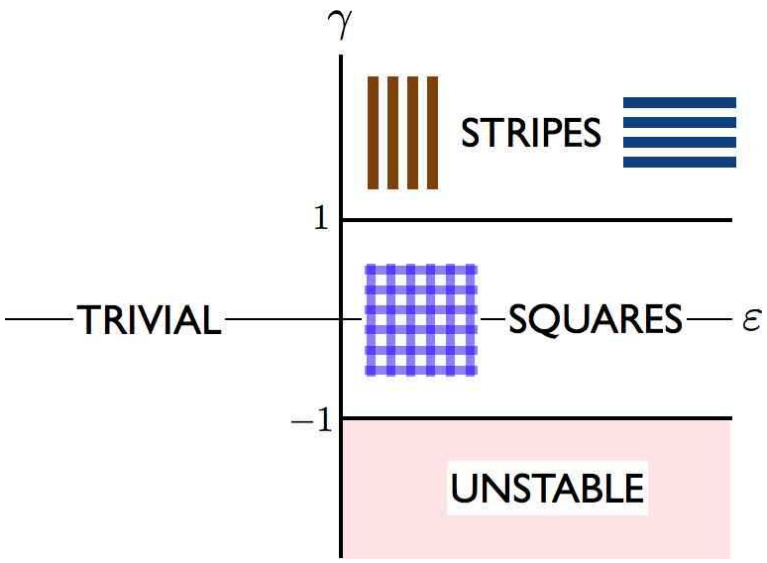

Figure 9.6: Phase diagram for the $M = 2$ system.

and

$$L_{\rm III} = \begin{pmatrix} (1-\gamma)\,\varepsilon & -2\gamma\,\varepsilon \\ 0 & -2\varepsilon \end{pmatrix} \quad , \quad L_{\rm IV} = -\frac{2\varepsilon}{1+\gamma}\begin{pmatrix} 1 & \gamma \\ \gamma & 1 \end{pmatrix} . \tag{9.104}$$

Computing $\mathcal{T} = {\rm Tr}(L)$ and $\mathcal{D} = \det(L)$, we find:

(I) In the trivial phase, we have $\mathcal{T} = 2\varepsilon$ and $\mathcal{D} = \varepsilon^2$. This fixed point is stable star if $\varepsilon < 0$ and an unstable star if $\varepsilon > 0$.[3]

(II) In the striped phase, we have $\mathcal{T} = -(1+\gamma)\,\varepsilon$ and $\mathcal{D} = 2(\gamma-1)\,\varepsilon^2$. Thus, if $\gamma < 1$ the stripes are unstable as the fixed point is a saddle. Now suppose $\gamma > 1$, meaning $\mathcal{D} > 0$. The fixed point is therefore stable since $\varepsilon > 0$. If $\varepsilon < 0$, there is no solution for the fixed point at all. We next compute $\mathcal{D} - \frac{1}{4}\mathcal{T}^2 = -\frac{1}{4}(\gamma-3)^2\,\varepsilon^2$ which is always negative, indicating that the fixed point is always a stable node.

(III) Same as case II.

(IV) We find $\mathcal{T} = -4\varepsilon/(\gamma+1)$ and $\mathcal{D} = 4\varepsilon^2\,(1-\gamma)/(1+\gamma)$. The condition $\mathcal{D} > 0$ is equivalent to $|\gamma| < 1$. For $|\gamma| > 1$, this fixed point is a saddle, and is unstable. Note that $|\mathcal{A}_{1,2}|^2 = -\mathcal{T}/4g$ at the fixed point, so if a solution exists we must have $\mathcal{T} < 0$. If $|\gamma| < 1$ then, the fixed point is stable, and we find $\mathcal{D} - \frac{1}{4}\mathcal{T}^2 = -4\varepsilon^2\gamma^2/(1+\gamma)^2 < 0$, indicating a stable node. Note that a fixed point solution exists for $\varepsilon < 0$ if $1+\gamma < 0$, which means $\gamma < -1$, which is a saddle and unstable.

The phase diagram is shown in fig. 9.6.

[3]The star is a nongeneric fixed point, arising here because the eigenspace is degenerate. Note that $\mathcal{D} = \frac{1}{4}\mathcal{T}^2$ for the type I case.

$M = 3$ case

For $M = 3$ we write

$$\hat{\boldsymbol{n}}_1 = \hat{\boldsymbol{x}} \quad , \quad \hat{\boldsymbol{n}}_2 = -\tfrac{1}{2}\,\hat{\boldsymbol{x}} + \tfrac{\sqrt{3}}{2}\,\hat{\boldsymbol{y}} \quad , \quad \hat{\boldsymbol{n}}_3 = -\tfrac{1}{2}\,\hat{\boldsymbol{x}} - \tfrac{\sqrt{3}}{2}\,\hat{\boldsymbol{y}} \ , \tag{9.105}$$

with $\boldsymbol{q}_j = Q\,\hat{\boldsymbol{n}}_j$, with $\hat{\boldsymbol{n}}_{r+3} = -\hat{\boldsymbol{n}}_\ell$. The σ field is then given by the sum

$$\sigma(\boldsymbol{r}, t) = A_1\,e^{i\boldsymbol{q}_1\cdot\boldsymbol{r}} + A_2\,e^{i\boldsymbol{q}_2\cdot\boldsymbol{r}} + A_3\,e^{i\boldsymbol{q}_3\cdot\boldsymbol{r}} + A_1^*\,e^{-i\boldsymbol{q}_1\cdot\boldsymbol{r}} + A_2^*\,e^{-i\boldsymbol{q}_2\cdot\boldsymbol{r}} + A_3^*\,e^{-i\boldsymbol{q}_3\cdot\boldsymbol{r}} \ . \tag{9.106}$$

Let's suppose the $\sigma \to -\sigma$ symmetry is broken, leaving us with the Haken model,

$$\frac{\partial\sigma}{\partial t} = \left[\varepsilon - \left(Q^2 + \boldsymbol{\nabla}^2\right)^2\right]\sigma + v\sigma^2 - \sigma^3 \ . \tag{9.107}$$

The resulting amplitude equations are then

$$\frac{dA_\ell}{dt} = \varepsilon\,A_\ell + v\,A_{\ell-1}^*\,A_{\ell+1}^* - g\,|A_\ell|^2 A_\ell - \gamma\,g\left(|A_{\ell-1}|^2 + |A_{\ell+1}|^2\right)A_\ell \ , \tag{9.108}$$

Our notation is cyclic in ℓ mod 3, so $A_{\ell+1} = A_1$ when $\ell = 3$, and $A_{\ell-1} = A_3$ when $\ell = 1$.

We now convert to amplitude and phase variables, writing

$$A_\ell = R_\ell\,e^{i\phi_\ell} \ . \tag{9.109}$$

Plugging this into the amplitude equations and taking the real part, we obtain

$$\frac{dR_\ell}{dt} = \varepsilon R_\ell + vR_{\ell-1}R_{\ell+1}\,\cos\phi - gR_\ell^3 - \gamma g\big(R_{\ell-1}^2 + R_{\ell+1}^2\big)R_\ell \tag{9.110}$$

where

$$\phi = \phi_1 + \phi_2 + \phi_3 \ . \tag{9.111}$$

The imaginary part yields the equations

$$\frac{d\phi_\ell}{dt} = -\frac{R_{\ell-1}R_{\ell+1}}{R_\ell}\cdot v\,\sin\phi \ . \tag{9.112}$$

Adding these last three equations, we obtain a single equation for the total phase angle ϕ:

$$\frac{d\phi}{dt} = -\frac{R_1^2\,R_2^2 + R_2^2\,R_3^2 + R_3^2\,R_1^2}{R_1R_2R_3}\cdot v\sin\phi \ . \tag{9.113}$$

Thus, $\sin\phi = 0$ is a fixed point for these dynamics, and in steady state, we have

$$\begin{aligned} v < 0 \quad &\Rightarrow \quad \phi = \pi \\ v > 0 \quad &\Rightarrow \quad \phi = 0 \ . \end{aligned}$$

Thus, $v\cos\phi > 0$ in steady state, *i.e.* $v\cos\phi = |v|$. Assuming the phase angle has reached its steady state value, the amplitude equations are given by

$$\frac{dR_1}{dt} = \varepsilon R_1 + |v| R_2 R_3 - g R_1^3 - \gamma g\big(R_2^2 + R_3^2\big) R_1 \tag{9.114}$$

$$\frac{dR_2}{dt} = \varepsilon R_2 + |v| R_3 R_1 - g R_2^3 - \gamma g\big(R_3^2 + R_1^2\big) R_2 \tag{9.115}$$

$$\frac{dR_3}{dt} = \varepsilon R_3 + |v| R_1 R_2 - g R_3^3 - \gamma g\big(R_1^2 + R_2^2\big) R_3 \ . \tag{9.116}$$

Subtracting the first equation from the second gives

$$\frac{d}{dt}\big(R_1 - R_2\big) = \Big[\varepsilon - |v| R_3 - g\big(R_1^2 + R_1 R_2 + R_2^2\big) - \gamma g R_3^2 + \gamma g R_1 R_2\Big]\big(R_1 - R_2\big) \ . \tag{9.117}$$

For sufficiently small ε, we suspect that the term in brackets is negative, indicating that the difference $R_1 - R_2$ tends to zero. As we could have chosen any two distinct values of r, we are motivated to consider the symmetric case $R_1 = R_2 = R_3 = R$. This results in the equation

$$\frac{dR}{dt} = \varepsilon R + |v| R^2 - g\,(1 + 2\gamma) R^3 \ . \tag{9.118}$$

The fixed points $\dot R = 0$ occur at $R = 0$ and at $R = R_\pm$, where

$$R_\pm = \frac{|v| \pm \sqrt{v^2 + 4\varepsilon\, g\,(1 + 2\gamma)}}{2g\,(1 + 2\gamma)} \ . \tag{9.119}$$

This solution describes a hexagonal structure.

To assess the stability of these solutions, it is *incorrect* to analyze the stability of eqn. 9.118. Rather, we must go back to the full $N = 4$ system (R_1, R_2, R_3, ϕ). Since the partial derivatives $\partial\dot R_\ell/\partial\phi = -v R_{\ell-1} R_{\ell+1}\sin\phi$ all vanish at the fixed point, we only need consider the $N = 3$ system (R_1, R_2, R_3) in eqns. 9.114, 9.115, and 9.116. We must examine the Jacobian

$$\begin{aligned} J_{\ell\ell'} = \frac{\partial\dot R_\ell}{\partial R_{\ell'}} &= \begin{pmatrix} a & b & b \\ b & a & b \\ b & b & a \end{pmatrix} \\ &= (a - b)\,\mathbb{I} + 3b\,|\psi\rangle\langle\psi| \ , \end{aligned} \tag{9.120}$$

where $\psi^{\rm t} = \frac{1}{\sqrt{3}}(1, 1, 1)$. Thus, $|\psi\rangle$ is an eigenvector with eigenvalue $\lambda_+ = a + 2b$, while the two-dimensional subspace orthogonal to $|\psi\rangle$ has the (doubly degenerate) eigenvalue $\lambda_- = a - b$. Thus,

$$\begin{aligned} \lambda_+ &= \varepsilon + 2|v| R - 3(1 + 2\gamma) g R^2 \\ &= -2\varepsilon - |v| R \end{aligned} \tag{9.121}$$

and

$$\begin{aligned}\lambda_- &= \varepsilon - |v|R - 3gR^2 \\ &= \frac{2}{1+2\gamma}\Big((\gamma-1)\,\varepsilon - (2+\gamma)\,|v|R\Big)\ .\end{aligned} \tag{9.122}$$

We have used the fixed point equation

$$g(1+2\gamma)\,R^2 - |v|R - \varepsilon = 0 \tag{9.123}$$

to eliminate the quadratic terms in R in these expressions for $\lambda_\pm$.

Consider the $R = R_+$ fixed point. Plugging the expression for R_+ into the expressions for $\lambda_\pm$, the stability criteria $\lambda_\pm < 0$ can be investigated. that the $R = R_+$ solution is stable for

$$-\frac{v^2}{4g(1+2\gamma)} \ < \ \varepsilon \ < \ \frac{(2+\gamma)\,v^2}{g(\gamma-1)^2}\ . \tag{9.124}$$

The lower limit for ϵ is set by the condition $\lambda_+ < 0$, and the upper limit by $\lambda_- < 0$. The $R = R_0$ solution and all other fixed points (such as when $v\cos\phi < 0$) are unstable. For example, there are so-called mixed modes, where

$$R_1 = \frac{|v|}{g\,(\gamma-1)} \qquad , \qquad R_2 = R_3 = \sqrt{\frac{\varepsilon - gR_1^2}{g\,(\gamma+1)}}\ . \tag{9.125}$$

These are also unstable.

The hexagonal pattern is described by

$$\sigma(\boldsymbol{r},t) = 2R(t)\Big[\cos(Q\,\hat{\boldsymbol{n}}_1\cdot\boldsymbol{r}+\phi_1) + \cos(Q\,\hat{\boldsymbol{n}}_2\cdot\boldsymbol{r}+\phi_2) \pm \cos(Q\,\hat{\boldsymbol{n}}_3\cdot\boldsymbol{r}-\phi_1-\phi_2)\Big]\ . \tag{9.126}$$

where the upper sign is taken when $v > 0$ ($\phi = 0$), and the lower sign when $v < 0$ ($\phi = \pi$). Let us define the primitive *reciprocal lattice vectors*

$$\boldsymbol{b}_1 = Q\,\hat{\boldsymbol{x}} \qquad , \qquad \boldsymbol{b}_2 = Q\left(\tfrac{1}{2}\hat{\boldsymbol{x}} + \tfrac{\sqrt{3}}{2}\,\hat{\boldsymbol{y}}\right)\ . \tag{9.127}$$

With this definition, we have

$$\begin{aligned}&\boldsymbol{q}_1 = \boldsymbol{b}_1 && \boldsymbol{q}_2 = \boldsymbol{b}_2 - \boldsymbol{b}_1 && \boldsymbol{q}_3 = -\boldsymbol{b}_2 \\ &\boldsymbol{q}_4 = -\boldsymbol{b}_1 && \boldsymbol{q}_5 = \boldsymbol{b}_1 - \boldsymbol{b}_2 && \boldsymbol{q}_6 = \boldsymbol{b}_2\ .\end{aligned}$$

We also define the primitive *direct lattice vectors*

$$\boldsymbol{a}_1 = \frac{4\pi}{\sqrt{3}\,Q}\big(\tfrac{\sqrt{3}}{2}\hat{\boldsymbol{x}} - \tfrac{1}{2}\hat{\boldsymbol{y}}\big) \qquad , \qquad \boldsymbol{a}_2 = \frac{4\pi}{\sqrt{3}\,Q}\,\hat{\boldsymbol{y}}\ . \tag{9.128}$$

Note that

$$\boldsymbol{a}_\mu\cdot\boldsymbol{b}_\nu = 2\pi\,\delta_{\mu\nu}\ . \tag{9.129}$$

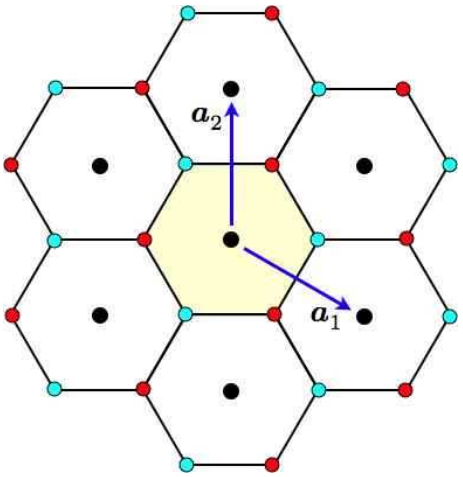

Figure 9.7: Points of high symmetry in the honeycomb lattice. The black dots label the Γ sublattice, the blue dots the K sublattice, and the red dots the K′ sublattice.

We can expand $\boldsymbol{r}$ in the basis of primitive direct lattice vectors as

$$\boldsymbol{r} \equiv \frac{\zeta_1}{2\pi}\,\boldsymbol{a}_1 + \frac{\zeta_2}{2\pi}\,\boldsymbol{a}_2 \ . \tag{9.130}$$

Then

$$\begin{aligned}\sigma(\boldsymbol{r},t) &= 2R(t)\Big[\cos\big(\boldsymbol{b}_1\cdot\boldsymbol{r}+\phi_1\big) + \cos\big((\boldsymbol{b}_2-\boldsymbol{b}_1)\cdot\boldsymbol{r}+\phi_2\big) \pm \cos\big(\boldsymbol{b}_2\cdot\boldsymbol{r}+\phi_1+\phi_2\big)\Big] \\ &= 2R(t)\Big[\cos\big(\zeta_1+\phi_1\big) + \cos\big(\zeta_2-\zeta_1+\phi_2\big) \pm \cos\big(\zeta_2+\phi_1+\phi_2\big)\Big] \ .\end{aligned} \tag{9.131}$$

If we now shift the origin of coordinates, defining

$$\tilde\zeta_1 = \begin{cases}\zeta_1+\phi_1 & \text{if } v>0\\ \zeta_1+\phi_1+\pi & \text{if } v<0\end{cases} \quad , \qquad \tilde\zeta_2 = \zeta_2+\phi_2 \ , \tag{9.132}$$

then we have

$$\sigma(\boldsymbol{r},t) = \pm 2R(t)\Big[\cos\tilde\zeta_1 + \cos\big(\tilde\zeta_2-\tilde\zeta_1\big) + \cos\tilde\zeta_2\Big] \ , \tag{9.133}$$

where again the upper sign is for $v>0$ and the lower sign for $v<0$. Consider the case $v>0$. At a fixed time t, the function $\sigma(\boldsymbol{r},t)$ achieves its maxima $\sigma_{\rm max}=6R$ when $\tilde\zeta_1=0$ modulo 2π and $\tilde\zeta_2=0$ modulo 2π, which is to say when $\boldsymbol{r}$ lies on a triangular lattice of points, which we call the Γ sublattice. This pattern is known as the H0 hexagonal pattern. The minima lie on a honeycomb lattice, which can be described as two interpenetrating triangular lattices. The K sublattice is defined by the set of points equivalent to $\tilde\zeta_1=\frac{4\pi}{3}$ and $\tilde\zeta_2=\frac{2\pi}{3}$, while the K′ sublattice consists of the points equivalent to $\tilde\zeta_1=\frac{2\pi}{3}$ and $\tilde\zeta_2=\frac{4\pi}{3}$, again modulo 2π in either component. The sum of the three cosines is then $-\frac{3}{2}$, hence $\sigma_{\rm min}=-3R$. For $v<0$ the roles of minima and maxima are reversed, and the maxima lie on the vertices of a honeycomb lattice; this is the Hπ structure. See figs. 9.7 and 9.8.

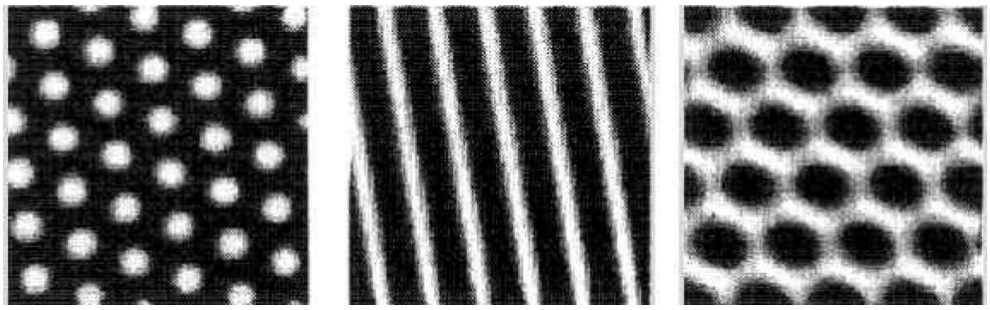

Figure 9.8: Two-dimensional stationary Turing patterns, showing H0 (left), striped (center), and Hπ (right) structures. White areas correspond to local maxima of the concentration field. From A. De Wit, *Adv. Chem. Phys.* **109**, 435 (1999).

Hexagons are not the only stable pattern, however. We can find stripe solutions where $R_1 = R$ and $R_2 = R_3 = 0$. Nontrivial solutions occur for $\varepsilon > 0$, where $R = \sqrt{\varepsilon/g}$, as in the one-dimensional case. The Jacobian at this fixed point is given by

$$J_{\ell\ell'} = \begin{pmatrix} -2\varepsilon & 0 & 0 \\ 0 & (1-\gamma)\,\varepsilon & |v|\sqrt{\frac{\varepsilon}{g}} \\ 0 & |v|\sqrt{\frac{\varepsilon}{g}} & (1-\gamma)\,\varepsilon \end{pmatrix} \quad . \tag{9.134}$$

The eigenvalues are $\lambda_1 = -2\varepsilon$ and $\lambda_{2,3} = (1-\gamma)\,\varepsilon \pm |v|\sqrt{\frac{\varepsilon}{g}}$. Since $\varepsilon > 0$ in order to have a nontrivial solution, $\lambda_1 < 0$ and we can focus on $\lambda_{2,3}$. If $\gamma < 1$ then $\lambda_2 > 0$, so stripes are unstable for $\gamma < 1$. If $\gamma > 1$, we have that $\lambda_3 < 0$, and the condition $\lambda_2 < 0$ requires

$$\varepsilon > \frac{v^2}{g(1-\gamma)^2} \tag{9.135}$$

for the stripes to be stable, along with $\gamma > 1$.

It is convenient to rescale, defining

$$|v| \equiv u \cdot \sqrt{4g(1+2\gamma)} \quad , \quad R \equiv S \cdot \frac{u}{\sqrt{g}} \quad , \quad \varepsilon \equiv \eta \cdot u^2 \ . \tag{9.136}$$

Then we find

$$S_{\rm HEX}(\eta) = \frac{1 \pm \sqrt{1+\eta}}{\sqrt{1+2\gamma}} \qquad , \qquad S_{\rm STRIPE}(\eta) = \sqrt{\eta} \ . \tag{9.137}$$

The upper solution for the hexagons is stable for $\eta_- < \eta < \eta_+$, whereas the stripe solution is stable for $\eta > \eta_{\rm s}$, where

$$\eta_- = -1 \qquad , \qquad \eta_{\rm s} = \frac{4\,(1+2\gamma)}{(\gamma-1)^2} \qquad , \qquad \eta_+ = \frac{4\,(1+2\gamma)\,(2+\gamma)}{(\gamma-1)^2} \ . \tag{9.138}$$

These results are plotted in fig. 9.9.

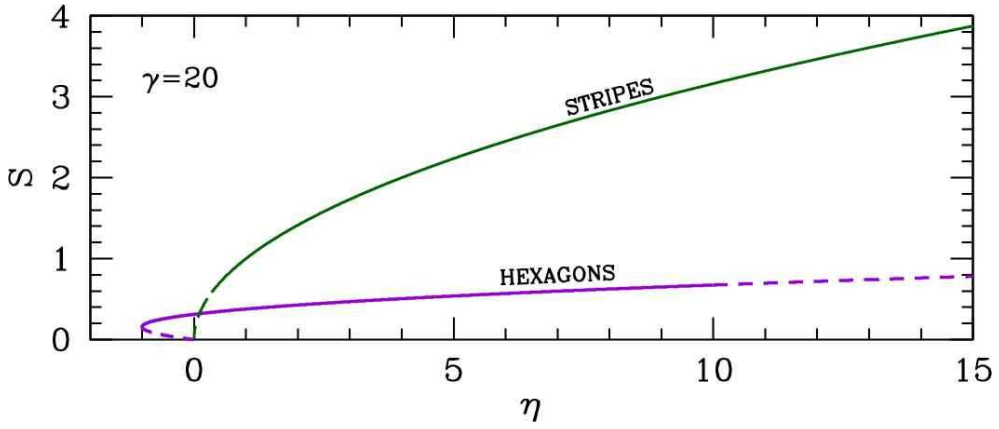

Figure 9.9: Dimensionless amplitude S *versus* dimensionless coupling η for the $M = 3$ system discussed in the text, showing stable (solid) and unstable (dashed) solutions.

9.5.4 $d = 3$

We can extend the previous $d = 2$ results to $d = 3$ dimensions simply by assuming there is no variation in the along z, the coordinate in the third direction. Thus, stripes in $d = 2$ become lamellae in $d = 3$. New structures emerge as well:

$$\begin{aligned} M = 3 \;:\; 2M = 6 \quad &\Rightarrow \text{ simple cubic in reciprocal and real space} \\ M = 4 \;:\; 2M = 8 \quad &\Rightarrow \text{ BCC reciprocal lattice, FCC direct lattice} \\ M = 6 \;:\; 2M = 12 \quad &\Rightarrow \text{ FCC reciprocal lattice, BCC direct lattice .} \end{aligned}$$

For a description of the many patterned structures which can form under these periodicities, see T. K. Callahan and E. Knobloch, *Nonlinearity* **10**, 1179 (1997) and *idem*, *Physica D* **132**, 339 (1999).

9.6 Anisotropy

Many physical systems exhibit intrinsic spatial anisotropies. To see how these might affect patterning, consider a modification of the Brusselator with anisotropic diffusion:

$$u_t = D_{u,\parallel}\, u_{xx} + D_{u,\perp}\, u_{yy} + a - (b+1)\, u + u^2 v \tag{9.139}$$

$$v_t = D_{v,\parallel}\, v_{xx} + D_{v,\perp}\, v_{yy} + b\, u - u^2 v \ . \tag{9.140}$$

The linearized dynamics, from eqn. 9.14, are given by the matrix

$$L(q) = \begin{pmatrix} b - 1 - \widetilde{D}_u(\phi)\, q^2 & a^2 \\ -b & -a^2 - \widetilde{D}_v(\phi)\, q^2 \end{pmatrix} \ . \tag{9.141}$$

where

$$q_x = q\cos\phi \qquad , \qquad q_y = q\sin\phi \tag{9.142}$$

and

$$\widetilde{D}_u(\phi) = D_{u,\parallel}\cos^2\phi - D_{u,\perp}\sin^2\phi \tag{9.143}$$

$$\widetilde{D}_v(\phi) = D_{v,\parallel}\cos^2\phi - D_{v,\perp}\sin^2\phi \ . \tag{9.144}$$

We identify the maximally unstable wavevector for the Turing instability $\det(L) = 0$ as before, *i.e.* by minimizing $\det(L)$ with respect to q^2. We then invoke $\det(L) = 0$, which gives us a second equation. From these two equations we obtain the critical value of b at the transition and the critical wavevector at the transition:

$$b_{\rm T}(\phi) = \left(1 + a\sqrt{\frac{\widetilde{D}_u(\phi)}{\widetilde{D}_v(\phi)}}\right)^2 \tag{9.145}$$

$$Q^2(\phi) = \frac{a}{\sqrt{\widetilde{D}_u(\phi)\,\widetilde{D}_v(\phi)}} \ . \tag{9.146}$$

We have thus described a one-parameter family of Turing instabilities, as a function of the angle ϕ. The earliest (smallest $b_{\rm T}(\phi)$ value) of these will preempt the others. Examining $b_{\rm T}(\phi)$, we find

$$\frac{D_{u,\perp}}{D_{u,\parallel}} > \frac{D_{v,\parallel}}{D_{v,\perp}} \quad \Rightarrow \quad \phi = 0 \tag{9.147}$$

$$\frac{D_{u,\perp}}{D_{u,\parallel}} < \frac{D_{v,\parallel}}{D_{v,\perp}} \quad \Rightarrow \quad \phi = \frac{\pi}{2} \ . \tag{9.148}$$

9.7 Phase Diffusion : Eckhaus and Zigzag Instabilities

Starting from the Swift-Hohenberg equation, the dynamics of a striped configuration, with $\sigma(x,y,t) = 2\,\mathsf{Re}\left[A(x,y,t)\,e^{iQx}\right]$ are governed by the Newell-Whitehead-Segel equation,

$$\frac{\partial A}{\partial T} = \mu\,A + \left(\frac{\partial}{\partial X} + \frac{i}{2}\frac{\partial^2}{\partial Y^2}\right)^2 A - |A|^2 A \ , \tag{9.149}$$

where X, Y, and T are scaled 'slow variables', $X = \varepsilon_0 Qx$, $Y = |\varepsilon_0|^{1/2}Qy$, $T = 4Q^2|\varepsilon_0|t$, and $\varepsilon = 4Q^2|\varepsilon_0|\,\mu$, where $|\varepsilon_0| \ll 1$. The amplitude has also been scaled by a factor of $\frac{2}{\sqrt{3}}Q^2|\varepsilon_0|^{1/2}$.

The optimal pattern is given by the constant solution $A = \sqrt{\mu}$, for $\mu > 0$, corresponding to $\sigma(x) = 2\sqrt{\mu}\cos(Qx)$. However, for $\varepsilon > 0$ an entire band of wavevectors is linearly unstable, since $\varepsilon - (Q^2 + \boldsymbol{\nabla}^2)^2$ acting on any plane wave $e^{i\boldsymbol{q}\cdot\boldsymbol{r}}$ will yield a positive growth rate so long

as $|q^2 - Q^2| < \sqrt{\varepsilon}$. Thus the Newell-Whitehead-Segel (NWS) equation admits a band of static solutions,

$$A(X,Y) = \sqrt{\mu - k^2}\; e^{ikX} \ , \tag{9.150}$$

for $|k| < \sqrt{\mu}$. We now investigate the stability of these solutions, writing

$$A(X,Y,T) = \left(\sqrt{\mu - k^2} + \rho(X,Y,T)\right) e^{ikX}\, e^{i\phi(X,Y,T)} \ , \tag{9.151}$$

and linearizing in the amplitude and phase variations ρ and ϕ.

We start by defining $\Lambda = kX + \phi$. Then

$$e^{-i\Lambda}\,\frac{\partial}{\partial X}\,e^{i\Lambda} = \frac{\partial}{\partial X} + ik + i\,\frac{\partial\phi}{\partial X} \tag{9.152}$$

$$e^{-i\Lambda}\,\frac{\partial}{\partial Y}\,e^{i\Lambda} = \frac{\partial}{\partial Y} + i\,\frac{\partial\phi}{\partial Y} \ . \tag{9.153}$$

Thus,

$$e^{-i\Lambda}\left(\partial_X - \tfrac{i}{2}\partial_Y^2\right)e^{i\Lambda} = ik + \partial_X - \tfrac{i}{2}\partial_Y^2 + i\phi_X + \tfrac{1}{2}\phi_{YY} + \phi_Y\partial_Y + \tfrac{i}{2}\phi_Y^2 \tag{9.154}$$

We need to square the RHS and then apply it to $\left(\sqrt{\mu - k^2} + \rho\right)$, and then keep only terms up to linear order in ρ, ϕ, and their derivatives. Clearly we can drop the last two terms on the RHS above since $\phi_Y\partial_Y$ will be nonzero only when acting on ρ or ϕ, resulting in a nonlinear contribution; the last term ϕ_Y^2 is already nonlinear. Even with the reduction from seven to five terms, squaring is a slightly tedious process, and we skip the intermediate steps. Multiplying the NWS equation on the left by $e^{-i\Lambda}$ and then collecting real and imaginary terms, we obtain the coupled equations

$$\rho_T = -2(\mu - k^2)\,\rho - 2k\sqrt{\mu - k^2}\;\phi_X + \rho_{XX} + k\,\rho_{YY} + \sqrt{\mu - k^2}\;\phi_{XYY} - \tfrac{1}{4}\,\rho_{YYYY} \tag{9.155}$$

$$\phi_T = \frac{2k}{\sqrt{\mu - k^2}}\,\rho_X + \phi_{XX} + k\,\phi_{YY} - \frac{1}{2\sqrt{\mu - k^2}}\,\rho_{XYY} - \tfrac{1}{4}\,\phi_{YYYY} \ . \tag{9.156}$$

The terms on the RHS of these equations are ordered by increasing powers of derivatives. We assume a long wavelength disturbance, meaning we can neglect all but the lowest nontrivial terms. From the RHS of the first equation, we take the first two terms, which yield

$$\rho = -\frac{k}{\sqrt{\mu - k^2}}\,\phi_X \ . \tag{9.157}$$

Note that $\rho \propto \phi_X$, which means that the LHS of the first equation is $\rho_T \propto \phi_{XT}$, which has one more derivative. Substituting this result into the second equation, we obtain

$$\phi_T = \left(\frac{\mu - 3k^2}{\mu - k^2}\right)\phi_{XX} + k\,\phi_{YY} \ . \tag{9.158}$$

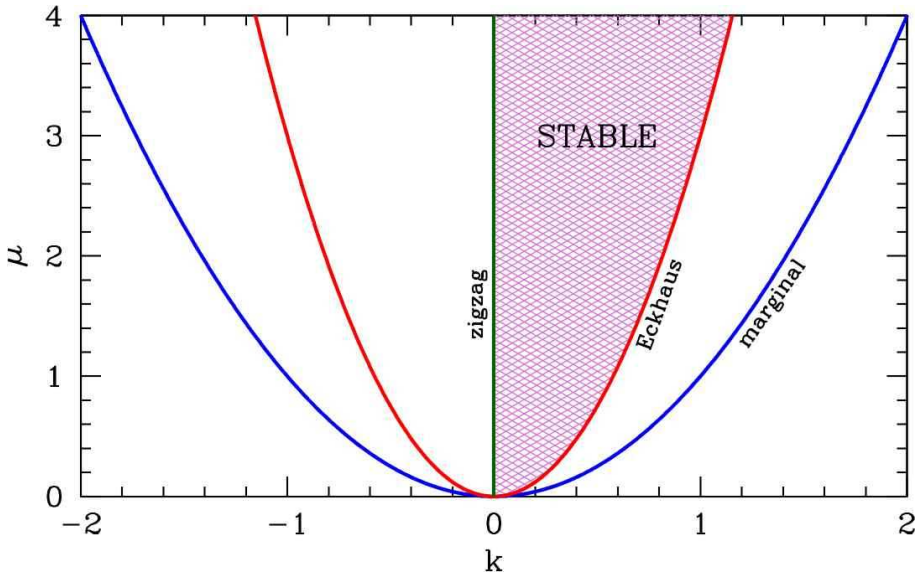

Figure 9.10: Boundary curves for Eckhaus and zigzag instabilities. Structures within the shaded region are stable.

This is an anisotropic diffusion equation. We identify

$$D_{\phi,X} = \frac{\mu - 3k^2}{\mu - k^2} \qquad , \qquad D_{\phi,Y} = k \ . \tag{9.159}$$

An instability occurs when either diffusion constant is negative. Note that $\mu = k^2$ is the so-called *marginal stability boundary* and that no patterned solution exists for $k^2 > \mu$. The condition $D_{\phi,X} < 0$ corresponds to the *Eckhaus instability* and $D_{\phi,Y} < 0$ to the *zigzag instability*. A sketch of the stability boundaries is provided in fig. 9.10.

These are many other patterning instabilities, several of which are discussed in detail in the book by R. Hoyle, listed in chapter 0 of these notes.